Published in final edited form as:
Cell Metab. 2013 August 6; 18(2): 239–250. doi:10.1016/j.cmet.2013.07.002.

Mitochondrial Complex I Deficiency Increases Protein Acetylation and Accelerates Heart Failure

Georgios Karamanlidis[1], **Chi Fung Lee**[1], **Lorena Garcia-Menendez**[1], **Stephen C. Kolwicz Jr**[1], **Wichit Suthammarak**[2,*], **Guohua Gong**[1], **Margaret M. Sedensky**[2], **Philip G. Morgan**[2], **Wang Wang**[1], and **Rong Tian**[1]

[1]Mitochondria and Metabolism Center, Department of Anesthesiology, University of Washington, Seattle, WA 98109, USA

[2]Children's Research Institute, Seattle, WA 98101, USA

Summary

Mitochondrial respiratory dysfunction is linked to the pathogenesis of multiple diseases including heart failure but the specific mechanisms for this link remain largely elusive. We modeled the impairment of mitochondrial respiration by inactivation of the *Ndufs4* gene, a protein critical for Complex I (C-I) assembly, in the mouse heart (cKO). While C-I supported respiration decreased by >40%, the cKO mice maintained normal cardiac function *in vivo* and high-energy phosphate content in isolated perfused hearts. However, the cKO mice developed accelerated heart failure after pressure overload or repeated pregnancy. Decreased NAD^+/NADH ratio by C-I deficiency inhibited Sirt3 activity, leading to increase in protein acetylation, and sensitization of the permeability transition in mitochondria (mPTP). NAD^+ precursor supplementation to cKO mice partially normalized the NAD^+/NADH ratio, protein acetylation and mPTP sensitivity. These findings describe a mechanism connecting mitochondrial dysfunction to the susceptibility to diseases and propose a potential therapeutic target.

Introduction

Mitochondrial dysfunction contributes to the pathogenesis of a wide variety of common diseases including neurodegenerative diseases, obesity, diabetes and cardiovascular diseases. Mitochondria-triggered cell death is a major cause of cardiac injury and heart failure during cardiac stress. Studies in mitochondrial diseases have shown that over 50% of individuals with mutations in genes encoding mitochondrial proteins develop cardiomyopathy, implicating the significance of mitochondrial defects in the development of cardiac pathology (DiMauro and Schon, 2003). Observations from human studies on heart failure as well as in animal models suggest that defects in mitochondrial bioenergetics may contribute to the development and progression of the disease. "Energy starvation" has been a longstanding hypothesis in the pathogenesis of heart failure; multiple defects in substrate metabolism, oxidative phosphorylation and energy transfer mechanisms have been suggested (Neubauer, 2007). Impairment of oxidative phosphorylation due to dysfunction in

Corresponding author: Rong Tian, MD, PhD, Tel: 206 543 8982, Fax: 206 616 4819, rongtian@u.washington.edu.
*Currently at the Department of Biochemistry, Faculty of Medicine Siriraj Hospital, Mahidol University, Bangkok, Thailand

The authors declare no conflict of interest.

the electron transport chain (ETC) not only affects ATP production but also has been proposed to impair intracellular Ca^{2+} flux, increase reactive oxygen species (ROS) generation, and alter redox balance due to changes in the NAD^+/NADH ratio (Grad et al., 2005; Neubauer, 2007).

Impaired function of complex I of the ETC has been observed in several diseases including cardiomyopathy and heart failure (Ide et al., 1999; Marin-Garcia et al., 2009; Scheubel et al., 2002). Complex I contains ~45 different subunits and its main role is to transfer electrons from NADH to the ETC for ATP synthesis. Under normal conditions it is estimated that up to 5% of the mitochondrial oxygen consumption can be converted into reactive oxygen species (ROS) as a byproduct of the ETC activity, primarily by complex I and III (Lee and Wei, 1997). ETC dysfunction is often associated with increased ROS generation and cellular damage in model systems, but the antioxidant treatment is far less effective in patients. On the other hand, cell death (both apoptosis and necrosis) due to the abnormal opening of the mitochondria permeability transition pore (mPTP) has been proposed as a disease mechanism in multiple diseases including heart failure (Elrod et al., 2010; Halestrap, 2010; Millay et al., 2008; Nakayama et al., 2007). Thus, identifying the molecular intermediaries linking the mitochondrial respiratory dysfunction with the mitochondria-triggered cell death is critical to advance our knowledge.

In the present study we sought to elucidate the role of impaired ETC function in the development of cardiac injury using a mouse model with cardiac-specific deletion of *Ndusf4* in complex I of the ETC. Our results show that impaired ETC activity due to decreased complex I function does not impair ATP supply or exacerbate ROS production under unstressed conditions. However, complex I deficiency leads to NADH accumulation and decreased NAD^+/NADH ratio, which inhibits Sirt3 activity and results in protein hyper-acetylation. This in turn renders the mice highly susceptible to additional stresses and accelerates the development of heart failure after chronic increases of workload.

Results

Deletion of *Ndufs4* reduced complex I assembly and function in cardiac mitochondria

Since global deletion of *Ndufs4* leads to premature death due to encephalopathy (Kruse et al., 2008), we deleted *Ndufs4* specifically in the heart to study the role of mitochondrial dysfunction in cardiac function. Cardiac-specific deletion of *Ndufs4* (cKO) in mice resulted in more than a 90% ($p<0.05$) decrease of the *Ndufs4* mRNA and protein levels at 3–4 months of age in the heart compared to littermate controls ($Ndufs4^{lox/lox}$, CON; Figure 1A–B). The expression of several complex I genes, i.e. NDUFB6, NDUFB8 and NDUFA9 remained unaltered at the mRNA level but was significantly reduced at the protein level. In contrast, the complex II protein SDHB, remained unchanged in the cKO hearts. The mRNA levels of several genes representative of the ETC complexes II–IV also remained unchanged (Figure 1A). Furthermore, microarray analysis of the cKO hearts did not reveal any significant mRNA changes more than 1.5 folds (FDR <0.05%) when compared to CON hearts, except the *Ndufs4* mRNA (Figure S1A). In-gel complex I activity assays using blue native gel (BNG) electrophoresis showed that complex I abundance in the monomeric form as well as in the super-complex assembly was significantly reduced (Figure S1B). Furthermore, a lower molecular weight band bearing NADH dehydrogenase activity was present in the cKO mitochondrial extracts, which likely represented the non-assembled or degraded product of complex I. Thus, deletion of *Ndufs4* in the heart did not change the gene expression of other mitochondrial proteins but promoted the degradation of complex I proteins. These data show that *Ndufs4* is essential for the assembly and/or stability of complex I, and that the loss of Ndufs4 protein resulted in a poorly assembled and fragile complex I.

Complex activities measured in isolated sub-mitochondrial particles showed a ~75% ($p<0.05$) decrease in complex I activity, whereas complex II and IV activities were not affected (Figure S1C). We also measured mitochondrial respiration and O_2 consumption in permeabilized cardiac myofibers to assess complex I function in the intact mitochondria. Complex I supported respiration was decreased by ~45% ($p<0.05$) in the cKO myofibers, which was also reflected in the complex I+II supported respiration, whereas complex II supported respiration was not affected (Figure 1C). Similar decreases in complex I activity and complex I supported respiration were also observed in cardiac mitochondria isolated from *Ndufs4*-null mice (global deletion), suggesting that the deletion of the *Ndufs4* in cKO heart is near complete (Figure S1D–E). Therefore, the lack of *Ndufs4* resulted in substantial but incomplete loss of complex I function in cardiac mitochondria. The greater impairment of complex I activity detected in the sub-mitochondrial particles of cKO was likely due to the instability of complex I that rendered it more vulnerable to degradation during the isolation process.

Normal lifespan and *in vivo* cardiac function in cardiac complex I deficient mice

To determine the long-term effects of decreased complex I activity on the heart, we monitored survival and *in vivo* cardiac function in cKO mice by echocardiography every 6 months for 30 months. As shown in Figure 1D, despite the impairment of complex I function, the cKO mice had a similar lifespan as the CON mice. No significant difference was observed in fractional shortening (FS%) or left ventricle (LV) chamber dimension at any age in the cKO mice (Figure 1E–F). We observed a small but statistically significant increase in the LV posterior wall thickness in the cKO mice at 18 and 24 months of age (Figure 1G). Similar observations were made in both male and female mice (Figure S1F–K). Tissue citrate synthase (CS) activity, a commonly used marker of mitochondrial mass, was similar between cKO and CON hearts (Figure 1H). Mitochondrial morphology and number also appeared normal in the cKO hearts compared to CON, as assessed by electron microscopy (Figure 1I–J). Thus, the significant complex I deficiency in cKO did not affect survival, cardiac function or mitochondrial stereological characteristics in unstressed mice.

Maintained myocardial energetics and LV performance in cKO hearts during dobutamine stimulation

To determine whether complex I deficiency affected ATP production and myocardial energetics, we measured dynamic changes of high energy phosphate content using ^{31}P NMR spectroscopy in isolated Langendorff-perfused hearts during dobutamine infusion. To test whether substrate preference would affect these responses, separate cohorts were perfused with a buffer containing primarily glucose or mixed substrates (i.e., glucose, fatty acids, and lactate). During baseline perfusion, the concentration of the energy reserve compound, phosphocreatine, (PCr), was slightly higher in cKO hearts perfused with a mixed substrate buffer (Figure 2A; $p<0.05$) and was similar in WT and cKO hearts perfused with glucose-based buffer (Figure S2A; $P=.0958$). The total creatine content was not different (Figure S2I). No significant differences were noted in inorganic phosphate ([Pi]) or ATP concentrations ([ATP]) between the genotypes perfused with either substrate mixture at baseline (Figure 2B–C; Figure S2B–C). At the end of the dobutamine challenge, [PCr] and [ATP] decreased to the same degree in both cKO and CON hearts perfused with either buffer. [Pi] increased further in cKO hearts after dobutamine challenge with the mixed substrate buffer, and there was also a trend for higher [Pi] with the glucose-based buffer. The change in Pi reflected the higher amount of PCr in cKO at baseline, which was depleted to the same level as CON during dobutamine challenge. Intracellular pH was constant throughout the perfusion protocol (Figure 2D, Figure S2D). Simultaneous assessment of cardiac function revealed that left ventricular developed pressure (LVDevP) and heart rate (HR) were not statistically different in cKO and CON during baseline perfusion regardless

of the substrates supplied in the perfusate (Figure 2E–F; Figure S2E–F). In response to dobutamine challenge, both cKO and CON had an equivalent ~2-fold increase in contractile performance assessed by rate-pressure product (RPP) which was primarily accomplished by significant increases in HR (Figure 2E–G; Figure S2E–G). Coronary flow also remained similar during the course of the experiment between the two groups (Figure 2H; Figure S2H). These observations suggest that the cKO heart is able to maintain normal myocardial energetics during baseline workload, and it is able to respond to acute increases of workload demand while sustaining myocardial energetics and contractile function.

Accelerated heart failure in cKO mice in response to chronic stress

We next tested whether complex I deficiency would affect the response to chronic cardiac stress. When we subjected mice to pressure overload by transverse aortic constriction (TAC), the cKO mice had an accelerated transition to heart failure (Figure 3A–D). The cKO mice displayed a significant decrease in FS% and a significant LV dilatation compared to CON mice as early as 2 weeks post TAC surgery. These changes persisted at 4 weeks after TAC. Heart weight and lung wet-weight, indices of congestive heart failure, were increased in both genotypes after TAC, but they were more prominent in the cKO mice compared to the CON littermates ($p<0.05$). To further confirm that this effect was specific to *Ndufs4* deletion and not due to overexpression of CRE recombinase in the mouse model, we subjected a group of CRE overexpressing mice to TAC surgery. Four weeks after TAC surgery CRE overexpressing mice had similar decreases in FS%, increases in LV dimension and heart weight as the CON-TAC mice, whereas these changes were exacerbated in the cKO-TAC mice (Figure S3A–C), suggesting that the overexpression of CRE recombinase *per se* did not contribute to the accelerated heart failure in this model.

Increased blood volume during pregnancy exerts volume overload on the heart causing physiological hypertrophy with full postpartum recovery in healthy individuals. In control female mice, we have not observed cardiac dysfunction due to repeated pregnancies for up to a year. Surprisingly, after 5–6 gestation cycles the cKO female mice developed cardiomyopathy, characterized by decreased FS% and significant LV dilatation compared to CON female mice that had gone through equal numbers of pregnancy (Figure 3E–I). Note that nulliparous female cKO mice had normal cardiac function at a similar age (12 months old; Figure S1). These observations show that the cKO mice are able to maintain cardiac function under unstressed conditions but are unable to adapt to chronic volume overload.

We also subjected mice to swim exercise for two 90-min sessions per day, 5 days/week for a total of 4 weeks (Kregel et al., 2006). We started with 10 mice per group; 7 CON mice and 8 cKO mice completed the study. At the end of 4 weeks of swim exercise the heart weight and citrate synthase enzyme activity in the gastrocnemious muscle were significantly increased in both genotypes compared to the sedentary groups (Figure S4A–B). Cardiac function *in vivo*, assessed by echocardiography, was decreased in the cKO mice, which was accompanied by an increase in LV chamber size (Figure S4C–D). Taken together, the results suggest that complex I function is essential for responding to chronic increases of workload due to either pathological or physiological causes.

Complex I deficiency enhanced mPTP sensitivity and increased cell death during chronic stress, which was not accounted for by increased ROS production

In cardiac tissue sections from cKO female breeders who had developed cardiomyopathy we found a 2-fold increase of TUNEL positive nuclei, increased fibrosis and increased cardiac myocyte size compared to heart sections from CON female mice with the same number of breeding cycles (Figure 4A–F). These results suggest that complex I deficiency triggered cell death during chronic stress. To determine if the cell death originated from abnormal

opening of the mPTP we isolated cardiac mitochondria from cKO and CON mice and performed mitochondrial swelling and Ca^{2+} uptake assays. Mitochondria from cKO hearts displayed accelerated swelling in response to Ca^{2+} loading compared to that from CON hearts, which was prevented by the addition of the mPTP blocker, Cyclosporin A (CsA; Figure 4G). In a parallel experiment we also measured Ca^{2+} uptake and the induction of the mPTP opening in isolated mitochondria. The mPTP opening could be triggered in mitochondria from the cKO hearts by a significantly lower amount of Ca^{+2} compared to CON mitochondria, and the opening event was prevented in both genotypes by the addition of CsA (Figure 4H). These findings collectively suggest that mitochondria from the cKO heart are more sensitive to Ca^{2+} challenge and more vulnerable to mPTP opening and cell death.

Excessive ROS production has been previously suggested to increase the mPTP sensitivity to Ca^{2+} challenge (Halestrap, 2010). Additionally, complex I dysfunction has been associated with increased ROS production in the aging heart (Petrosillo et al., 2009). However, H_2O_2 production was not increased in the cKO mitochondria compared to CON under any of the conditions we tested (Figure 5A). In contrast, we found that complex I mediated H_2O_2 production (by forward or reverse electron flow through complex I) was decreased in the cKO mitochondria compared to CON. Furthermore, we found that mitochondrial but not cytosolic H_2O_2 production was significantly decreased in isolated cardiomyocytes from cKO using fluorescent probes of H_2O_2 targeted to mitochondrial or cytosolic compartments in cardiomyocytes (Figure 5B). Consistently, superoxide level in cKO was also lower in permeabilized cardiomyocytes both at baseline and after pyruvate/malate/ADP (P/M/ADP) stimulated respiration (Figure 5C–D). Aconitase activity, which is sensitive to oxidative damage, was similar between the two genotypes (Figure 5E). In summary, these data support the notion that in cKO hearts complex I dependent electron transport is decreased because of decreased amounts of properly assembled complex and not due to complex I dysfunction (electron leakiness). We found no evidence of increased ROS production in cKO mitochondria. To further exclude the possibility that the cKO hearts had increased ROS production *in vivo* during stress, we crossed cKO mice with mice overexpressing mitochondrial targeted catalase (mCat; Figure 5F). Overexpression of mCat has been previously shown to protect against ROS damage (Dai et al., 2009). Overexpression of mCat in the cKO mice however, did not alter the course of heart failure induced by TAC surgery (Figure 5G–I). Taken together, these findings show that increased susceptibility to chronic stress in cKO is independent of oxidative stress.

Complex I deficiency led to decreased NAD^+/NADH ratio, increased protein acetylation and sensitized mPTP

Complex I is the major site for NADH oxidation. Hence we hypothesized that decreased function of complex I would result in NADH accumulation and an altered redox state in the mitochondria of the cKO hearts. Indeed, NADH was significantly increased in the cKO hearts with no change of NAD^+ levels, resulting in a ~50% decrease of the NAD^+/NADH ratio (Figure 6A). There were no changes in NADPH and $NADP^+$ levels (Figure S5A). The increase of the NAD pool is accompanied by an upregulation in the expression of the rate-limiting enzyme in NAD biosynthesis, Nampt (Figure S5B). To determine whether such a change in NAD^+/NADH ratio would affect Sirt3 activity, we tested the deacetylase activity of purified Sirt3 recombinant protein supplemented with fixed amount of NAD^+ and variable amounts of NADH. NADH exhibited a strong and dose-dependent inhibition of Sirt3 activity despite the fact that NAD^+ was constant (Figure 6B). Similar inhibition by NADH was also observed with Sirt2 (Figure S5C). Consistent with the finding that Sirt3 activity was inhibited by a lower NAD^+/NADH ratio, we found that mitochondrial protein extracts from the cKO hearts were hyper-acetylated (Figure 6C–D). Furthermore,

mitochondrial protein acetylation was also elevated in cKO mice that developed heart failure due to multiple gestation cycles (Figure S5D–E). The protein levels of the three mitochondrial localized sirtuins, Sirt3/4/5, were similar in cKO and CON (Figure S5F). Furthermore, the deacetylase activity of Sirt4/5, if any, was several orders of magnitude lower compared to Sirt3 (Figure S5G) suggesting that the inhibition of Sirt3 activity by a lower NAD^+/NADH ratio rather than changes in the expression of sirtuins or the activity of Sirt4/5 in the cKO was responsible for the increased acetylation. We also immunoprecipitated acetylated mitochondrial proteins from CON and cKO mitochondria and blotted for known Sirt3 targets, SOD2, NDUFA9 and SDHA (Figure S6H). Acetylation of NDUFA9 and SDHA was increased in the cKO mitochondria while SOD2 acetylation was unchanged suggesting that increased mitochondrial protein acetylation occurred in a subgroup of Sirt3 substrates in the cKO hearts. Overexpression of Sirt3 in cKO cardiac myocytes normalized the protein acetylation status (Figure 6E–F) as well as the sensitivity of mPTP opening (Figure 6G–H).

We next sought to alter the mitochondrial protein acetylation status by manipulating the NAD^+/NADH ratio both *in vitro* and *in vivo*. We first measured NADH fluorescence during different respiratory states in isolated cKO mitochondria (Figure 7A). NADH was increased in state-2 respiration with glutamate/malate (G/M), when NADH production was high relative to the ETC flux. The transition to state-3 after the addition of ADP reduced the NADH levels, because NADH was utilized for ATP synthesis. The addition of rotenone blocked complex I activity and increased the NADH levels. Based on this observation, we were able to reduce mitochondrial protein acetylation by pre-treatment of mitochondria with ADP and to increase protein acetylation by adding G/M, or rotenone and nicotinamide (NAM; Figure 7B–C). NAM is a potent inhibitor of Sirt3 activity in isolated mitochondria and was used as a positive control (Avalos et al., 2005). Simultaneous measurements of mitochondria calcium uptake and retention capacity showed that the sensitivity of the mPTP opening to calcium challenge followed the changes in the protein acetylation status (Figure 7D–E). To test the hypothesis *in vivo*, we sought to normalize the NAD^+/NADH ratio by treating the cKO mice with nicotinamide mononucleotide (NMN), an NAD precursor that has been previously shown to increase the intracellular NAD^+ levels (Yoshino et al., 2011). NMN supplementation for 3 days increased the NAD^+/NADH ratio in the cKO hearts, decreased the mitochondrial protein acetylation and improved the sensitivity of the mPTP in the cKO mitochondria (Figure 7F–I). Together, these results established a strong link between NAD^+/NADH ratio, mitochondrial protein acetylation and mPTP sensitivity, connecting the respiratory function of mitochondria to cell survival via protein acetylation.

Discussion

We demonstrate that deletion of *Ndufs4* results in significant loss of complex I supported respiration in the heart which is well tolerated with no major changes of cardiac function, energetics and longevity of the mice under unstressed conditions. Complex I deficiency, however, increases protein acetylation by altering the redox state, and renders the heart vulnerable to cell death and heart failure during chronic increases of workload. These findings describe a novel mechanism by which impaired mitochondrial complex I function predisposes the myocardium to injury via altered protein acetylation and susceptibility to chronic stress.

Deletion of *Ndufs4* resulted in a drastic reduction of complex I activity in sub-mitochondrial particles while mitochondrial respiration using complex I substrates in permeabilized cardiac myofibers was less affected. The dissociation between complex I supported respiration and its enzymatic activity in sub-mitochondrial particles has been previously reported in liver mitochondria from the *Ndufs4*-null mice as well as in MEF cells from the

same mice (Kruse et al., 2008; Valsecchi et al., 2012). Our study shows that the deletion of *Ndufs4* resulted in degradation of multiple proteins in complex I and failure to assemble supercomplexes suggesting that *Ndufs4* is critical for complex I assembly/stability. The "loosely" assembled complex I in the absence of *Ndufs4* makes it more vulnerable to mechanical dissociation during the isolation of sub-mitochondrial particles hence exaggerating the decrease of complex I activity. Using complex I substrate supported respiration in the intact mitochondria as a measurement of respiratory capacity we have determined that cardiac mitochondria of the cKO have approximately 50% of the normal complex I function.

Despite the decrease in complex I function, we did not observe any impairment in cardiac function or energetics in isolated isovolumic hearts from the cKO mice. Although, the workload of an isovolumic perfused heart experiments is lower than *in vivo* conditions, the heart responds normally to dobutamine stimulation by increasing contractile performance while sustaining myocardial high-energy phosphate content. A similar decrease in Complex I function but normal cardiac function under unstressed conditions has also been reported in the *Ndufs4* KO mice by a different group (Sterky et al., 2012). The same group also reported that MEF cells from Ndufs4-deficient mice had a >50% decrease in complex I supported respiration but the ATP production was not affected (Valsecchi et al., 2012). Thus, cardiac tissue has a remarkable reserve in complex I dependent ATP synthesis, and is able to tolerate a substantial loss of the function without affecting energetics in unstressed mice. This is in contrast to the brain where a similar impairment of complex I function lead to severe neurological defects and premature death in *Ndufs4*-null mice (Kruse et al., 2008; Quintana et al., 2010).

Complex I is a major source for mitochondrial ROS production in the ETC and certain pathological conditions have been shown to further enhance mitochondrial ROS production (Liu et al., 2002; McLennan and Degli Esposti, 2000). Dysfunctional complex I can generate more ROS due to the "leakiness" in the ETC. However, this is unlikely the case in mitochondria lacking *Ndufs4*, which based on our assessment, produce less superoxide or H_2O_2 under conditions of either forward or reverse electron flow. Moreover, overexpression of a potent antioxidant, catalase, targeted to mitochondria, did not improve the response to pressure overload in cKO mice. Although our study has not assessed every type and source of ROS, the results suggest that the pathogenic mechanisms for heart failure in this model are unlikely attributable to increased oxidative stress. These findings also support the notion that deletion of *Ndufs4* resulted in a loss of function rather than a dysfunctional complex I.

Although the complex I capacity is in excess for normal myocardial energetic demand at basal state, it is essential for maintaining mitochondrial redox state and for adaptation to chronic stress. The present study shows that complex I deficiency decreases the NAD^+/NADH ratio and impairs protein deacetylation. Changes in NAD^+/NADH ratio have been increasingly recognized as important regulatory mechanisms of physiological functions and diseases. For example, an increased NAD^+/NADH ratio has been proposed as an important mechanism mediating the beneficial effects of caloric restriction in health and longevity (Lin et al., 2004). In contrast, decreased NAD^+/NADH ratio has been observed in diabetes and obesity, and proposed as a disease mechanism (Ido, 2007). NAD^+ is a substrate for the class III NAD^+ dependent deacetylase Sirtuins, and a powerful activator of the Sirtuin activity (Avalos et al., 2005). Here we found that both Sirt2 and Sirt3 activities were inhibited with increasing NADH concentrations at a fixed amount of NAD^+. Competitive inhibition of the yeast Sir2 activity by NADH has also been previously shown (Lin et al., 2004). Among the 7 members of the Sirtuin family Sirt3 is specifically localized to mitochondria and has emerged as a major regulator of mitochondrial protein acetylation, whereas two other mitochondrial localized Sirtuins, Sirt4/5, have minimal deacetylase activity (Du et al., 2011;

He et al., 2012; Lombard et al., 2007). Since the protein level of Sirt3/4/5 is unaltered, our results suggest that inhibition of Sirt3 activity by a low NAD^+/NADH ratio causes mitochondrial protein hyper-acetylation in complex I deficient cardiac tissue. In support of this, restoration of the NAD^+/NADH ratio by NMN reduced mitochondrial protein acetylation in the cKO hearts.

The NAD^+/NADH ratio has been suggested to modulate the opening of the mPTP. NADH has been shown to bind to VDAC, which is an important regulator of the mPTP and alters the permeability of the mitochondrial outer membrane (Halestrap, 2010; Zizi et al., 1994). Recent studies have demonstrated that increased mitochondrial protein acetylation due to Sirt3 deletion is associated with increased sensitivity of mPTP opening (Hafner et al., 2010; Shulga and Pastorino, 2010; Shulga et al., 2010). Mice lacking Sirt3 have normal cardiac function but are sensitive to cardiac stress, resembling the observations reported here in mice with complex I deficiency in the heart (Hafner et al., 2010; Shulga and Pastorino, 2010; Shulga et al., 2010). In Sirt3 knockout mice, one study attributed increased cell death during stress to hyperacetylation of cyclophilin D and increased vulnerability of mPTP opening. We, however, failed to observe the hyperacetylation of cyclophilin D in *Ndufs4* cKO mice. Similarly, the acetylation of SOD2 did not change in cKO but increased significantly in Sirt3 null mice. These observations suggest that inhibition of sirtuin activity due to impaired mitochondrial function, unlike the deletion of Sirt3, does not uniformly affect its targets. However, other Sirt3 targets, e.g. NDUFA9 and SDHA, are hyperacetylated in cKO hearts. Moreover, overexpression of Sirt3 corrected protein hyper-acetylation and mPTP sensitivity in cKO cardiomyocytes. The evidence collectively suggests that increased mitochondrial protein acetylation is a common mechanism for the impaired response to cardiac stress. Furthermore, we have demonstrated that decreased NAD^+/NADH ratio and increased mitochondrial protein acetylation is causally linked to increased sensitivity of mPTP during calcium challenge. It remains however, to be determined whether it is the hyper-acetylation of a single protein or a select of protein targets that contributes to the increased sensitivity to cardiac stress. The similarities in the cardiac phenotype between the Ndufs4 cKO and the Sirt3 KO mice are intriguing but additional discrete mechanisms may also contribute to the phenotype.

In summary, the study identifies a novel mechanism that links mitochondrial respiratory function with protein modification and a cell death mechanism. The findings indicate that complex I dependent respiratory capacity is in excess of normal demand in cardiac mitochondria, and is partially dispensable for ATP production. It is, however, a critical regulator of the redox balance in the mitochondria, which is indispensable for cardiac response to chronic stress.

Experimental Procedures

Animal experiments and generation of *Ndufs4* KO mice

All animal experiments were performed with the approval of the Institutional Animal Care and Use Committee of the University of Washington. Mice were maintained on rodent diet and water available ad libitum in a vivarium with a 12 hr light/dark cycle at 22°C. To generate a cardiac restricted complex I deficient mouse, we crossed C57BL6 mice bearing the modified *ndufs4* gene containing loxP sites with transgenic C57BL6 mice expressing the enzyme CRE recombinase driven under the αMHC promoter. To generate cKOmCat mice, cKO mice were crossed with transgenic C57BL6 mice expressing the enzyme catalase targeted to mitochondria also driven under the αMHC promoter. For the nicotinamide mononucleatotide (NMN) experiment, mice at ~4 months old were administered with NMN (Sigma) intraperitoneally (i.p.) at 500mg/kg twice in three days. The hearts were harvested for mitochondria isolation and subsequent assays 24 hours after the last injection. Detailed

procedures for transverse aortic constriction, swimming exercise and echocardiography can be found in supplemental experimental procedures.

Mitochondrial isolation

Mitochondria were isolated as previously described (Boehm et al., 2001).

Polarography assays

Oxygen consumption of permeabilized cardiac myofibers by a Clark electrode was performed as described (Kuznetsov et al., 2008). Procedures are described in detail in supplemental experimental procedures.

Determination of mRNA and protein levels and immunoprecipitation (IP)

The isolation of total RNA. microarray analysis, real time PCR and immunoblot were described in supplemental experimental procedures. IP were performed with prewashed anti-acetyl-lysine antibody agarose (Immunechem). Detailed description can be also found in supplemental experimental procedures.

Biochemical assays

Enzyme activities were measured in isolated mitochondria solubilized in Cellytic buffer (Sigma). Citrate synthase (CS) and complex I, II and IV enzyme activities were measured as described (Kerner et al., 2001; Rockl et al., 2007; Yen et al., 1999). NAD^+/NADH as well as $NADP^+$/NADPH were measured using commercially available kits (BioAssay Systems). The aconitase enzyme activity was measured using an Aconitase Assay Kit (Cayman) according to manufacturer's instructions. The total creatine level was measured as previously described (Tian et al., 1996). Sirt3/4/5 activities *in vitro* were determined as described in Supplemental experimental procedures.

Histology and electron microscopy

In-depth description of the procedures of histology and electron microscopy of heart tissues is available in Supplemental experimental procedures.

Blue native gel (BNG) electrophoresis and complex I-In-gel activity staining

BNGs were performed as previously described (Suthammarak et al., 2009; Wittig et al., 2006) with minor modifications. Procedures are described in detail in supplemental experimental procedures.

Detection of H_2O_2 and superoxide production

The rate of H_2O_2 production in intact mitochondria was determined using the oxidation of the fluorogenic indicator amplex red in the presence of horseradish peroxidase (Moghaddas et al., 2003). In a typical experiment, 30 μg of mitochondria in a 96-well plate were incubated at 30°C and H_2O_2 production was initiated in mitochondria by the addition of the substrates indicated in the respective figure.

For measurements of H_2O_2 production in intact cells, freshly isolated cardiac myocytes were plated on 25 mm coverslips coated with laminin (20 μg/mL) for 2 hr to allow for cell attachment. Attached myocytes were infected with adenovirus carrying Hyper (Cyto-Hyper, indicates cytosolic hydrogen peroxide) or mitochondrial-targeted Hyper (Mito-Hyper, indicates mitochondrial hydrogen peroxide) at an MOI of 100. Myocytes were cultured in M199 medium (Sigma) supplemented with 0.02% BSA, 5 mM creatine, 2 mM L-carnitine, 5 mM taurine, 5 mM HEPES, and insulin-transferrin-selenium-X. Myocytes were kept in

culture for 48 hr to allow adequate indicator expression prior to imaging. The basal level of cell Mito-Hyper or Cyto-Hyper was the average fluorescence ratio (488/405) of the first ten images.

For superoxide measurements, isolated cardiomyocytes were loaded with MitoSOX red (5 μM, for 10 min) and then permeabilized using saponine (50 μg/ml). Sequential 2-D confocal images were taken at 405 nm excitation, and emission was collected at >560 nm. Respiration was stimulated by adding 10 mM pyruvate, 5 mM malate and 2 mM ADP after the baseline scan. To calculate the rate of MitoSOX signal change (dF/dt), fluorescent signals during a 5-min period before or after the respiration stimulation were used.

Mitochondrial swelling and Ca^{2+} uptake assays

Mitochondrial swelling was induced in cardiac isolated mitochondria as previously described with minor modifications (Wang et al., 2005). In brief 200μg of mitochondria were incubated in a 96-well plate with 10mM of succinate with or without 1μM of Cyclosporin A (CsA) or 1 μM rotenone in 200 μl of swelling buffer (containing in mM: 120 KCl, 10 Tris-HCl (pH 7.4), 20 MOPS, and 5 KH_2PO_4) at 30°C. Swelling was initiated by additions of 25 μM Ca^{2+} and measured spectrophotometrically as a reduction in absorbance at 540 nm. Mitochondrial Ca^{2+} uptake assays were performed as we previously described to determine the Ca^{2+} retention capacity (Marcu et al., 2012).

Overexpression of Sirt3 and assessment of mPTP sensitivity in the intact cardiomyocytes

Determination of mPTP sensitivity in intact myocytes followed previously reported method (Zorov et al., 2000). Detailed description is available in Supplemental experimental procedures.

Isolated perfused mouse heart preparation and ^{31}P NMR spectroscopy

To assess left ventricular function and energetics, Langendorff isolated heart preparations were combined with ^{31}P nuclear magnetic resonance (NMR) spectroscopy (Kolwicz and Tian, 2010; Luptak et al., 2007; Yan et al., 2009). Procedures are described in detail in supplemental experimental procedures.

Statistical analysis

Comparisons among the groups were performed by 1-way ANOVA, followed by Tukey's post hoc comparisons. All analyses were performed using GraphPad Prism 4.0. All data are expressed as mean ± SEM and a $p<0.05$ was considered significant.

Supplementary Material

Refer to Web version on PubMed Central for supplementary material.

Acknowledgments

We thank Dr. Brian Hawkins and Dr. Raluca Marcu for developing the mitochondrial Ca^{2+} uptakes assays, Dr. Lisa Heather for the cardiac myofiber respiration assay, and Dr. Richard Palmiter and Dr. Peter Rabinovitch for providing the conditional Ndufs4 mice and the mitochondria targeted catalase mice. This study was supported by grants from the NHLBI (HL110349 and HL067970 to RT and HL114760 to WW), from the AHA (Scientist Development Grant to WW, Postdoctoral Fellowship to CFL), and from the NIA (to MS and PM).

References

Avalos JL, Bever KM, Wolberger C. Mechanism of sirtuin inhibition by nicotinamide: altering the NAD(+) cosubstrate specificity of a Sir2 enzyme. Molecular cell. 2005; 17:855–868. [PubMed: 15780941]

Boehm EA, Jones BE, Radda GK, Veech RL, Clarke K. Increased uncoupling proteins and decreased efficiency in palmitate-perfused hyperthyroid rat heart. American journal of physiology. 2001; 280:H977–983. [PubMed: 11179038]

Dai DF, Santana LF, Vermulst M, Tomazela DM, Emond MJ, MacCoss MJ, Gollahon K, Martin GM, Loeb LA, Ladiges WC, et al. Overexpression of catalase targeted to mitochondria attenuates murine cardiac aging. Circulation. 2009; 119:2789–2797. [PubMed: 19451351]

DiMauro S, Schon EA. Mitochondrial respiratory-chain diseases. The New England journal of medicine. 2003; 348:2656–2668. [PubMed: 12826641]

Du J, Zhou Y, Su X, Yu JJ, Khan S, Jiang H, Kim J, Woo J, Kim JH, Choi BH, et al. Sirt5 is a NAD-dependent protein lysine demalonylase and desuccinylase. Science (New York, N Y. 2011; 334:806–809.

Elrod JW, Wong R, Mishra S, Vagnozzi RJ, Sakthievel B, Goonasekera SA, Karch J, Gabel S, Farber J, Force T, et al. Cyclophilin D controls mitochondrial pore-dependent Ca(2+) exchange, metabolic flexibility, and propensity for heart failure in mice. The Journal of clinical investigation. 2010; 120:3680–3687. [PubMed: 20890047]

Grad LI, Sayles LC, Lemire BD. Introduction of an additional pathway for lactate oxidation in the treatment of lactic acidosis and mitochondrial dysfunction in Caenorhabditis elegans. Proceedings of the National Academy of Sciences of the United States of America. 2005; 102:18367–18372. [PubMed: 16344465]

Hafner AV, Dai J, Gomes AP, Xiao CY, Palmeira CM, Rosenzweig A, Sinclair DA. Regulation of the mPTP by SIRT3-mediated deacetylation of CypD at lysine 166 suppresses age-related cardiac hypertrophy. Aging. 2010; 2:914–923. [PubMed: 21212461]

Halestrap AP. A pore way to die: the role of mitochondria in reperfusion injury and cardioprotection. Biochemical Society transactions. 2010; 38:841–860. [PubMed: 20658967]

He W, Newman JC, Wang MZ, Ho L, Verdin E. Mitochondrial sirtuins: regulators of protein acylation and metabolism. Trends in endocrinology and metabolism: TEM. 2012; 23:467–476. [PubMed: 22902903]

Ide T, Tsutsui H, Kinugawa S, Utsumi H, Kang D, Hattori N, Uchida K, Arimura K, Egashira K, Takeshita A. Mitochondrial electron transport complex I is a potential source of oxygen free radicals in the failing myocardium. Circulation research. 1999; 85:357–363. [PubMed: 10455064]

Ido Y. Pyridine nucleotide redox abnormalities in diabetes. Antioxidants & redox signaling. 2007; 9:931–942. [PubMed: 17508915]

Kerner J, Turkaly PJ, Minkler PE, Hoppel CL. Aging skeletal muscle mitochondria in the rat: decreased uncoupling protein-3 content. Am J Physiol Endocrinol Metab. 2001; 281:E1054–1062. [PubMed: 11595663]

Kolwicz SC Jr, Tian R. Assessment of cardiac function and energetics in isolated mouse hearts using 31P NMR spectroscopy. J Vis Exp. 2010

Kregel, CK.; Allen, DL.; Booth, FWRFM.; Henriksen, EJ.; Musch, TI.; O'Leary, DS.; Parks, CM.; Poole, DC.; Ra'anan, AW., et al. Resource Book for the Design of Animal Exercise Protocols. American Physiological Society; 2006.

Kruse SE, Watt WC, Marcinek DJ, Kapur RP, Schenkman KA, Palmiter RD. Mice with mitochondrial complex I deficiency develop a fatal encephalomyopathy. Cell metabolism. 2008; 7:312–320. [PubMed: 18396137]

Kuznetsov AV, Veksler V, Gellerich FN, Saks V, Margreiter R, Kunz WS. Analysis of mitochondrial function in situ in permeabilized muscle fibers, tissues and cells. Nature protocols. 2008; 3:965–976.

Lee HC, Wei YH. Role of Mitochondria in Human Aging. Journal of biomedical science. 1997; 4:319–326. [PubMed: 12386380]

Lin SJ, Ford E, Haigis M, Liszt G, Guarente L. Calorie restriction extends yeast life span by lowering the level of NADH. Genes & development. 2004; 18:12–16. [PubMed: 14724176]

Liu Y, Fiskum G, Schubert D. Generation of reactive oxygen species by the mitochondrial electron transport chain. Journal of neurochemistry. 2002; 80:780–787. [PubMed: 11948241]

Lombard DB, Alt FW, Cheng HL, Bunkenborg J, Streeper RS, Mostoslavsky R, Kim J, Yancopoulos G, Valenzuela D, Murphy A, et al. Mammalian Sir2 homolog SIRT3 regulates global mitochondrial lysine acetylation. Molecular and cellular biology. 2007; 27:8807–8814. [PubMed: 17923681]

Luptak I, Yan J, Cui L, Jain M, Liao R, Tian R. Long-term effects of increased glucose entry on mouse hearts during normal aging and ischemic stress. Circulation. 2007; 116:901–909. [PubMed: 17679614]

Marcu R, Neeley CK, Karamanlidis G, Hawkins BJ. Multi-parameter Measurement of the Permeability Transition Pore Opening in Isolated Mouse Heart Mitochondria. J Vis Exp. 2012:e4131. In press.

Marin-Garcia J, Goldenthal MJ, Damle S, Pi Y, Moe GW. Regional distribution of mitochondrial dysfunction and apoptotic remodeling in pacing-induced heart failure. Journal of cardiac failure. 2009; 15:700–708. [PubMed: 19786259]

McLennan HR, Degli Esposti M. The contribution of mitochondrial respiratory complexes to the production of reactive oxygen species. Journal of bioenergetics and biomembranes. 2000; 32:153–162. [PubMed: 11768748]

Millay DP, Sargent MA, Osinska H, Baines CP, Barton ER, Vuagniaux G, Sweeney HL, Robbins J, Molkentin JD. Genetic and pharmacologic inhibition of mitochondrial-dependent necrosis attenuates muscular dystrophy. Nature medicine. 2008; 14:442–447.

Moghaddas S, Hoppel CL, Lesnefsky EJ. Aging defect at the QO site of complex III augments oxyradical production in rat heart interfibrillar mitochondria. Archives of biochemistry and biophysics. 2003; 414:59–66. [PubMed: 12745255]

Nakayama H, Chen X, Baines CP, Klevitsky R, Zhang X, Zhang H, Jaleel N, Chua BH, Hewett TE, Robbins J, et al. Ca2+- and mitochondrial-dependent cardiomyocyte necrosis as a primary mediator of heart failure. The Journal of clinical investigation. 2007; 117:2431–2444. [PubMed: 17694179]

Neubauer S. The failing heart--an engine out of fuel. The New England journal of medicine. 2007; 356:1140–1151. [PubMed: 17360992]

Petrosillo G, Matera M, Moro N, Ruggiero FM, Paradies G. Mitochondrial complex I dysfunction in rat heart with aging: critical role of reactive oxygen species and cardiolipin. Free radical biology & medicine. 2009; 46:88–94. [PubMed: 18973802]

Quintana A, Kruse SE, Kapur RP, Sanz E, Palmiter RD. Complex I deficiency due to loss of Ndufs4 in the brain results in progressive encephalopathy resembling Leigh syndrome. Proceedings of the National Academy of Sciences of the United States of America. 2010; 107:10996–11001. [PubMed: 20534480]

Rockl KS, Hirshman MF, Brandauer J, Fujii N, Witters LA, Goodyear LJ. Skeletal muscle adaptation to exercise training: AMP-activated protein kinase mediates muscle fiber type shift. Diabetes. 2007; 56:2062–2069. [PubMed: 17513699]

Scheubel RJ, Tostlebe M, Simm A, Rohrbach S, Prondzinsky R, Gellerich FN, Silber RE, Holtz J. Dysfunction of mitochondrial respiratory chain complex I in human failing myocardium is not due to disturbed mitochondrial gene expression. J Am Coll Cardiol. 2002; 40:2174–2181. [PubMed: 12505231]

Shulga N, Pastorino JG. Ethanol sensitizes mitochondria to the permeability transition by inhibiting deacetylation of cyclophilin-D mediated by sirtuin-3. Journal of cell science. 2010; 123:4117–4127. [PubMed: 21062897]

Shulga N, Wilson-Smith R, Pastorino JG. Sirtuin-3 deacetylation of cyclophilin D induces dissociation of hexokinase II from the mitochondria. Journal of cell science. 2010; 123:894–902. [PubMed: 20159966]

Sterky FH, Hoffman AF, Milenkovic D, Bao B, Paganelli A, Edgar D, Wibom R, Lupica CR, Olson L, Larsson NG. Altered dopamine metabolism and increased vulnerability to MPTP in mice with

partial deficiency of mitochondrial complex I in dopamine neurons. Human molecular genetics. 2012; 21:1078–1089. [PubMed: 22090423]

Suthammarak W, Yang YY, Morgan PG, Sedensky MM. Complex I function is defective in complex IV-deficient Caenorhabditis elegans. The Journal of biological chemistry. 2009; 284:6425–6435. [PubMed: 19074434]

Tian R, Nascimben L, Kaddurah-Daouk R, Ingwall JS. Depletion of energy reserve via the creatine kinase reaction during the evolution of heart failure in cardiomyopathic hamsters. Journal of molecular and cellular cardiology. 1996; 28:755–765. [PubMed: 8732503]

Valsecchi F, Monge C, Forkink M, de Groof AJ, Benard G, Rossignol R, Swarts HG, van Emst-de Vries SE, Rodenburg RJ, Calvaruso MA, et al. Metabolic consequences of NDUFS4 gene deletion in immortalized mouse embryonic fibroblasts. Biochimica et biophysica acta. 2012

Wang G, Liem DA, Vondriska TM, Honda HM, Korge P, Pantaleon DM, Qiao X, Wang Y, Weiss JN, Ping P. Nitric oxide donors protect murine myocardium against infarction via modulation of mitochondrial permeability transition. American journal of physiology. 2005; 288:H1290–1295. [PubMed: 15528225]

Wittig I, Braun HP, Schagger H. Blue native PAGE. Nature protocols. 2006; 1:418–428.

Yan J, Young ME, Cui L, Lopaschuk GD, Liao R, Tian R. Increased glucose uptake and oxidation in mouse hearts prevent high fatty acid oxidation but cause cardiac dysfunction in diet-induced obesity. Circulation. 2009; 119:2818–2828. [PubMed: 19451348]

Yen HC, Oberley TD, Gairola CG, Szweda LI, St Clair DK. Manganese superoxide dismutase protects mitochondrial complex I against adriamycin-induced cardiomyopathy in transgenic mice. Archives of biochemistry and biophysics. 1999; 362:59–66. [PubMed: 9917329]

Yoshino J, Mills KF, Yoon MJ, Imai S. Nicotinamide mononucleotide, a key NAD(+) intermediate, treats the pathophysiology of diet- and age-induced diabetes in mice. Cell metabolism. 2011; 14:528–536. [PubMed: 21982712]

Zizi M, Forte M, Blachly-Dyson E, Colombini M. NADH regulates the gating of VDAC, the mitochondrial outer membrane channel. The Journal of biological chemistry. 1994; 269:1614–1616. [PubMed: 7507479]

Highlights

- Mitochondrial complex I deficiency decreases the NAD^+/NADH ratio in the heart
- Decreased NAD^+/NADH ratio inhibits Sirt3 leading to protein hyper-acetylation
- Protein hyper-acetylation in mitochondria sensitizes permeability transition pore
- Mitochondrial dysfunction raises heart susceptibility by redox sensitive mechanisms

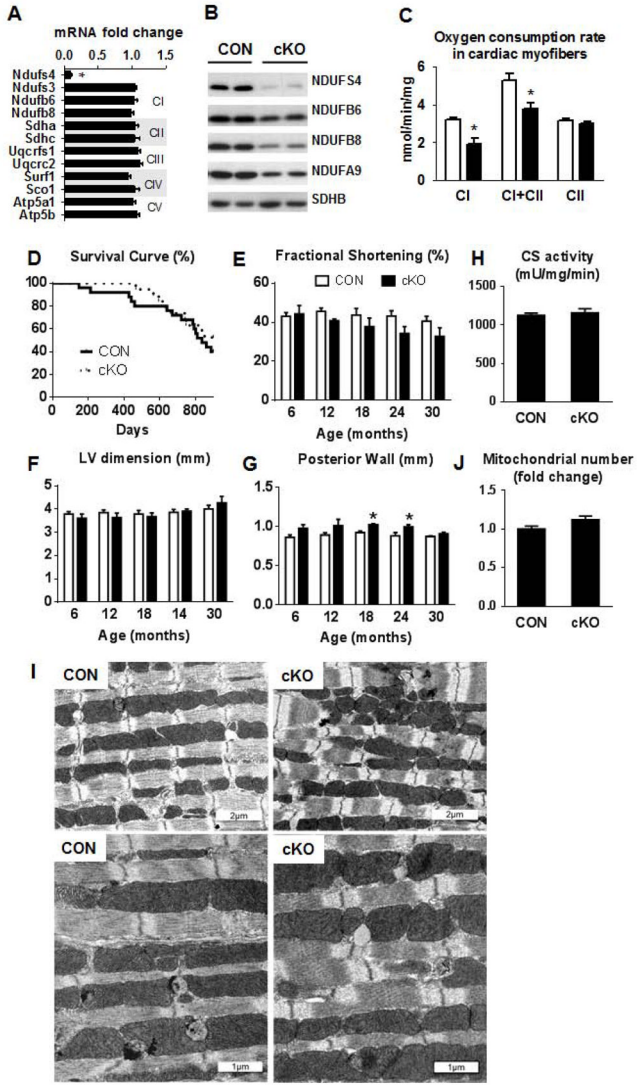

Figure 1. Mouse survival, cardiac function and mitochondrial assessment in Ndufs4 deficient mice

(**A**) Fold changes ±SEM of ETC gene expression in the cKO mice relative to CON (n=7). (**B**) Representative western blot for ETC proteins (n=4). (**C**) Mitochondrial state 3 respiration in permeabilized cardiac fibers. Pyruvate + malate was used as complex I substrate in the presence of ADP, then succinate was added to establish complex I + complex II (CI+CII) respiration and finally rotenone was added to block complex I and establish complex II (CII) respiration (mean ±SEM; n=3). (**D**) Kaplan-Meier survival curve of cKO and CON mice (n=19–25). Echocardiographic data depicting (**E**) fractional shortening (%), (**F**) LV end-diastolic dimension (mm) and (**G**) posterior wall thickness (mm) in CON (white) and cKO (black) mice over 30 months (n=6–13). (**H**) Cardiac tissue citrate synthase enzyme activity (n=13–15). Data are expressed as means ± SEM. *P<0.05 *vs* CON. (**I**) Electron microscopy images illustrating mitochondrial arrangement and morphological characteristic and (**J**) fold differences in total mitochondrial number. *P<0.05 *vs* CON. See also Figure S1 and Table S1.

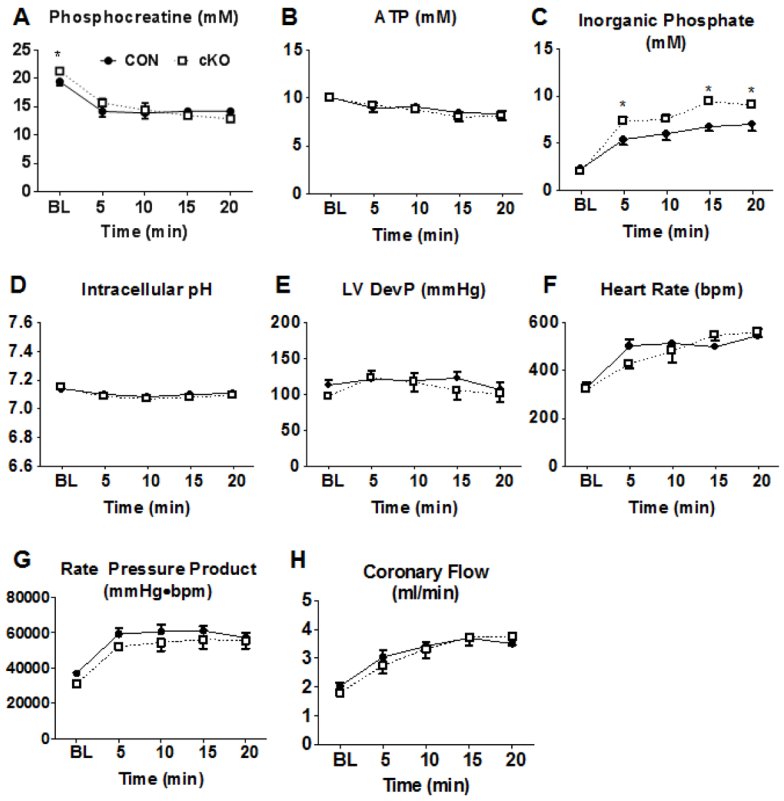

Figure 2. Myocardial energetics and cardiac function in isolated perfused hearts

(**A**) Phosphocreatine (PCr), (**B**) ATP, and (**C**) inorganic phosphate measured by ^{31}P NMR spectroscopy in isolated hearts perfused with mixed substrate buffer during normal workload and dobutamine challenge conditions. (**D**) Intracellular pH calculated from the chemical shift between PCr and Pi in isolated hearts perfused with mixed substrate buffer during normal workload and dobutamine challenge conditions. (**E**) Left ventricular developed pressure (LVDevP), (**F**) heart rate (HR), and (**G**) rate-pressure product (RPP), the product of LVDevP and HR, measured in isolated hearts perfused with mixed substrate buffer during normal workload and dobutamine challenge conditions. (**H**) Coronary flow, estimated by collecting the perfusate effluent over a 2-minute period, in Langendorff heart preparations during normal workload and dobutamine challenge conditions (n=5). Data are expressed as means ± SEM. *P<0.05 *vs* CON. See also Figure S2.

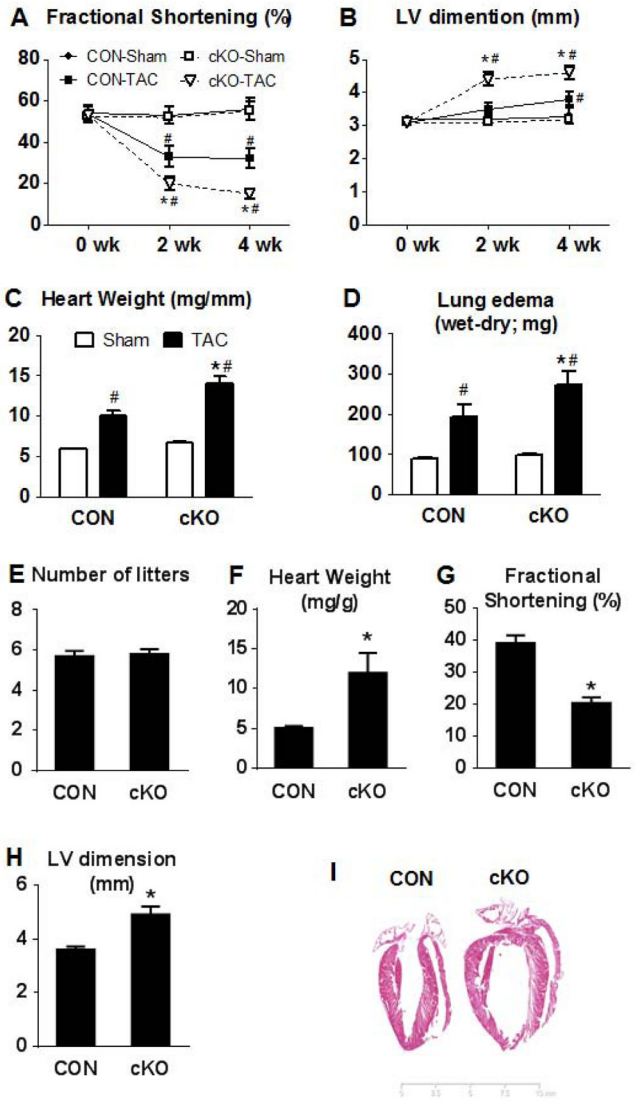

Figure 3. Cardiac function in response to cardiac stress

(**A**) Fractional shortening and (**B**) LV end-diastolic dimension before surgery (0wk) and at 2 or 4 weeks after TAC or sham surgery in male mice ($^{\#}P<0.05$ *vs* the respective sham group and $*P<0.05$ *vs* CON-TAC group). (**C**) Heart weight normalized to tibia length and (**D**) lung edema index at 4 weeks after TAC or sham surgery (n=5–6 sham and n=8–13 TAC). (**E**) Average number of litters for female CON and cKO mice, (**F**) heart weight normalized to body weight and (**H**) fractional shortening of these mice (n=9 CON and n=13 cKO; $*P<0.05$ *vs* CON). (**I**) H&E stain of a typical CON and cKO heart after 6 gestational cycles. Data are expressed as means ± SEM. See also Figures S3–4.

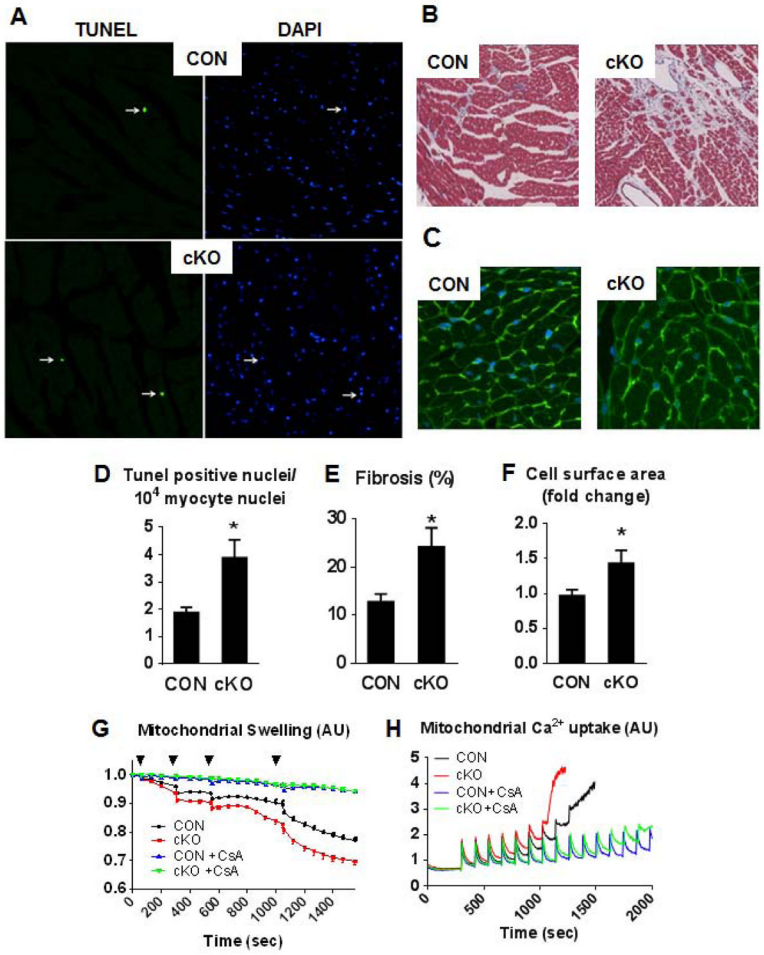

Figure 4. Increased cell death in the cKO hearts

Representative image of (**A**) TUNEL and DAPI stain for apoptotic nuclei, (**B**) trichrome stain for fibrosis and (**C**) WGA stain to outlining the cell surface area in female CON and cKO mice after 6 gestational cycles and quantitation graphs of those (**D–F**; n=4 per group, *P<0.05 *vs* CON). (**G**) Mitochondrial swelling induced by Ca^{2+} pulsing (25 μM [Ca^{2+}] increments in the reaction buffer) indicated by the black triangle measured as % decrease in the initial optical density (OD 540) in the presence or absence of 1 μM CsA (this experiment was repeated at least 5 times). (**H**) Representative Ca^{2+} uptake traces by mitochondria in the presence or absence of 1 μM CsA. Ca^{2+} was added to achieve 15 μM [Ca^{2+}] increments in the reaction buffer (this experiment was repeated at least 3 times). Data are expressed as means ± SEM.

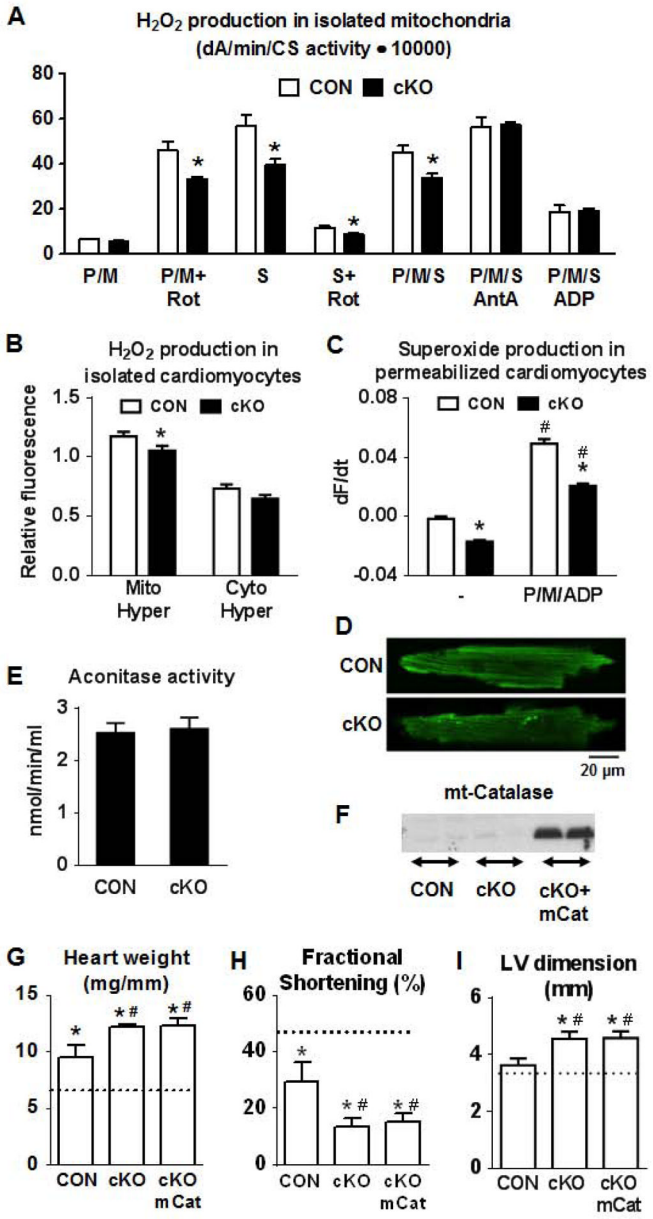

Figure 5. ROS production is not increased in the cKO hearts

(**A**) Measurement of H_2O_2 production using Amplex Red in isolated cardiac mitochondria from CON (white) and cKO (black) mice treated with pyruvate/malate (10/5 mM; P/M), succinate (10 mM; S), rotenone (10 μM; Rot), Antimicyn A (1 mg/ml; AntA), ADP (2.5 mM) or combinations of those (n=4) and (**B**) mitochondrial or cytosolic H_2O_2 production in isolated cardiomyocytes using a fluorescent probe targeted to mitochondria (Mito-Hyper) or to cytosol (Cyto-Hyper; n=27–43; *P<0.05 *vs* CON). (**C**) Data showing the change of MitoSOX fluorescence at 405 nm excitation during a 5 min period before (−) or after the addition of respiration substrates (P/M/ADP). Data are expressed as mean ± SEM (n=9–10 cells from 2–3 mice; #P<0.05 P/M/ADP vs. non-treated; *P< 0.05 cKO vs. CON). (**D**) Representative images of CON and cKO permeabilized cardiomyocytes showing the MitoSOX fluorescence at 5 min after the addition of respiration substrates (10 mM pyruvate, 5 mM malate and 2 mM ADP). (**E**) Cardiac tissue aconitase enzyme activity (n=3). Data are

expressed as means ± SEM. (**F**) Representative western blot for mitochondrial catalase in hearts from CON, cKO and cKO/mCat mice. (**G**) Heart weight normalized to tibia length, (**H**) fractional shortening and (**I**) LV end-diastolic dimension at 4 weeks after TAC or sham surgery (n=11 for the cKO/mCat TAC group and n=5 for the rest of the groups). Data are expressed as means ± SEM. *P<0.05 *vs* the respective sham indicated by the dotted line and $^{\#}$P<0.05 *vs* CON-TAC.

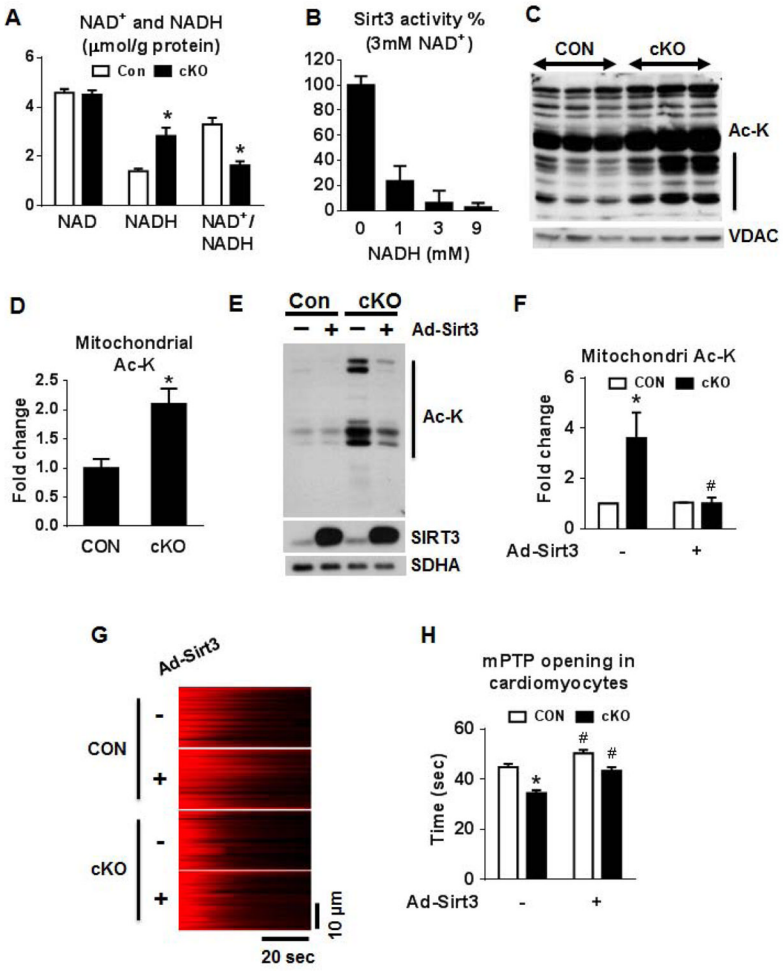

Figure 6. NAD$^+$/NADH regulates mitochondrial protein acetylation via SIRT3

(**A**) NADH and NAD$^+$ concentrations in freeze-clamped mouse hearts from CON and cKO mice (n=5). (**B**) Sirt3 activity assay using a 3 mM of NAD$^+$ and 0–9 mM of NADH. (**C**) Representative blot for acetylated lysine residues (Ac-K) and VDAC (loading control), and (**D**) a quantitation graph in cardiac mitochondrial extracts (n=4; vertical line in graph C indicates the area on the blot used for quantitation). (**E**) Western blot and (**F**) a quantitation graph of Ac-K residues in isolated cardiomyocytes from CON and cKO hearts overexpressing Sirt3. SIRT3 protein levels and SDHA (loading control) are also shown (n=3). (**G**) Representative linescan confocal images showing the laser induced mPTP opening in cultured adult cardiac myocytes as reflected by the sudden loss of membrane potential (TMRM, red color). (**H**) Summarized data showing the time from the start of scan to the mPTP opening (mPTP time), the shorter the time the more sensitive of the mPTP. n = 120–143 mitochondria from 21–25 cells isolated from 3 hearts in each group. All data are expressed as means ± SEM. *P<0.05 versus Con. $^{\#}$P<0.05 versus without AdSirt3. See also Figures S5.

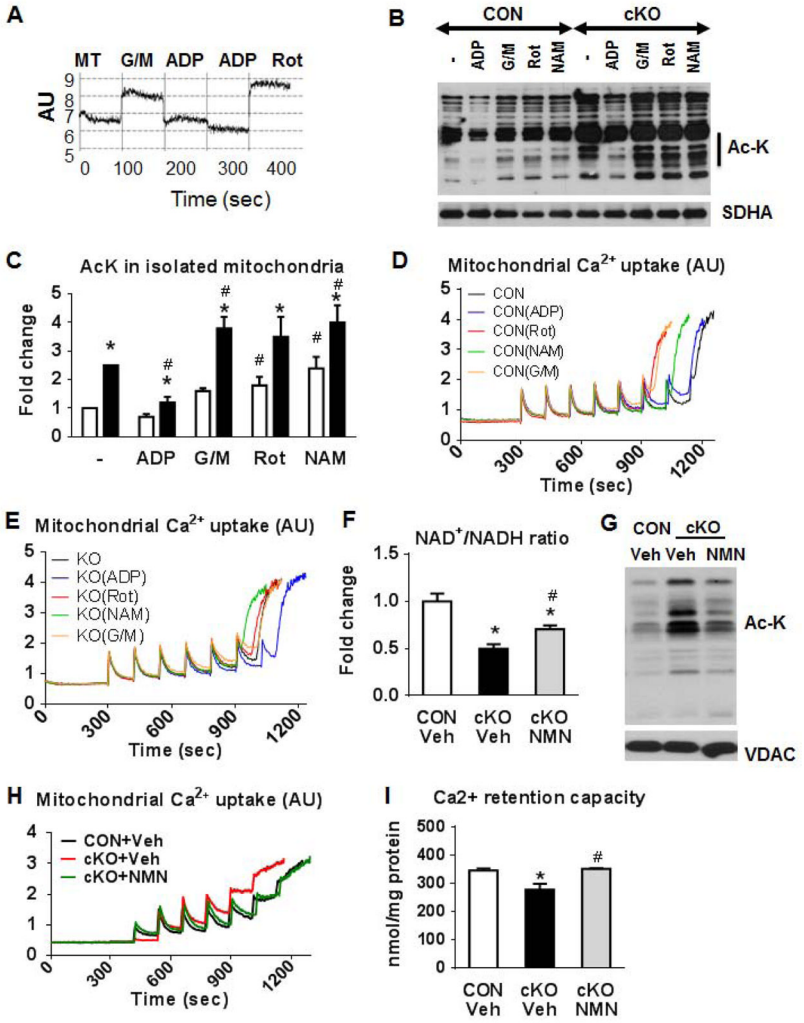

Figure 7. Regulation of the mPTP by mitochondrial NADH and protein acetylation

(**A**) Representative NADH autofluorescence trace using isolated mitochondria stimulated with glutamate/malate (G/M; 10/5 mM), ADP (250 μM) or Rot (1 μM) added in this order consecutively in the same trace. (**B**) A representative western blot and (**C**) a quantitation graph for Ac-K residues in protein extracts of CON and cKO mitochondria pre-treated separately with G/M (10/5 mM), or ADP (250 μM), or Rot (1 μM) or nicotinamide (NAM; 10 mM) for 20 min at 30°C (vertical line in graph B indicates the area on the blot used for quantitation), SDHA was used as loading controls. *P<0.05 *vs* CON non-treated and #P<0.05 *vs* cKO non-treated. Representative Ca^{2+} uptake traces from (**D**) CON and (**E**) cKO mitochondria, isolated in the presence or absence of G/M (10/5 mM), ADP (250 μM), Rot (1 μM) or NAM (10 mM). Each experiment was repeated at least 3 times. (**F**) NAD^+/NADH ratio in freeze-clamped mouse hearts from CON and cKO mice treated with vehicle or cKO treated with nicotinamide mononucleotide (NMN) as described in Methods (n=3). (**G**) Representative Western blots for Ac-K residues and VDAC (loading control) in CON and cKO cardiac mitochondria from mice treated with vehicle or NMN. (**H**) Ca^{2+} uptake traces and (**I**) quantitation graph from cardiac mitochondria isolated from CON and cKO mice treated with vehicle or NMN. Data in Panels F and I are expressed as means ± SEM. *P<0.05 *vs* CON-Veh and #P<0.05 *vs* cKO-Veh.